Available online at www.sciencedirect.com

ScienceDirect

Energy Procedia 123 (2017) 235–242

Energy Procedia

www.elsevier.com/locate/procedia

1st International Conference on Sustainable Energy and Resource Use in Food Chains, ICSEF 2017, 19-20 April 2017, Berkshire, UK

Reducing energy consumption in spray drying by monodisperse droplet generation: modelling and simulation

James C. Atuonwu[a,b]*, Andrew G. F. Stapley[a]

[a]*Department of Chemical Engineering, Loughborough University, Loughborough LE11 3TU United Kingdom*
[b]*Brunel University London, Institute of Energy Futures, Center for Sustainable Energy Use in Food Chains, Uxbridge, Middlesex UB8 3PH, UK*

Abstract

The possibilities of reducing energy consumption in spray drying by monodisperse droplet generation have been explored. From heat/mass balances and droplet travel dynamics in a single-stream spray dryer, correlations have been established for the drying gas temperatures that satisfy given outlet product moisture contents for droplet streams of different diameters–with skimmed milk as a case study. The results suggest that energy consumption can be reduced by up to 90%, compared to what obtains in a conventional system that produces droplet sizes up to 10 times the desired size. An experimental single-stream monodisperse droplet dryer, based on piezoelectric atomisation has been constructed, with an imaging system for future validation studies.

Peer-review under responsibility of the scientific committee of the 1st International Conference on Sustainable Energy and Resource Use in Food Chains.

Keywords: Spray drying; monodisperse droplet; energy savings; mathematical model; food processing

1. Introduction

Drying is a widely-applied energy-intensive process, accounting for 10-25% of overall industrial energy consumption in the developed world [1]. Spray drying, the primary method for producing dry powders from liquid feeds is a significant energy sink in for instance, milk production plants [2]. With the increasing strain on the fast-

* Corresponding author. Tel.: +441895268975;
E-mail address: james.atuonwu@brunel.ac.uk

1876-6102
Peer-review under responsibility of the scientific committee of the 1st International Conference on Sustainable Energy and Resource Use in Food Chains.
10.1016/j.egypro.2017.07.251

Nomenclature

C_D	Drag coefficient
C_p	Specific heat capacity (J/kg K)
D	Droplet diameter (m)
f	Droplet generation frequency (Hz)
G	Drying gas mass flowrate (kg/s)
g	Gravitational acceleration (9.81 m/s^2)
h	Heat transfer coefficient (W/m^2 K)
h_{fg}	Specific latent heat of vaporisation (kJ/kg)
M	Mass (kg)
q	Volumetric flowrate (m^3/s)
Q	Heat energy rate (J/s)
$S_{\%}$	Percentage energy savings
T	Temperature (°C)
U_{loss}	Dryer body heat loss coefficient (W/m^2 K)
U_p	Droplet velocity (m/s)
X	Moisture content dry basis (kg/kg)
Y	Drying gas absolute humidity dry basis (kg/kg)
z	Droplet/particle travel distance dimension (m)

Greek letters

α, β, γ, λ, φ, ω	Model fit parameters
ρ	Density (kg/m^3)

Subscripts

amb	Ambient
cr	Critical
d	Dry matter (milk)
D	Dryer
EQ	Equilibrium
G	Drying gas
in	Inlet, input
or	Orifice
p	Droplet/particle
ref	Reference
v	Water vapour
w	Liquid water

depleting global energy resources, stringent environmental regulations and high energy costs, innovative steps are needed to reduce spray drying energy consumption. Atomization has been regarded as the heart of the spray drying process [3] as it is inextricably linked to not only the drying kinetics and quality of the final product, but also to the energy efficiency of the process. Conventional spray dryers suffer from wide droplet size distributions of the atomised sprays. As droplet drying rate is proportional to its area per-unit volume, larger-diameter droplets imply lower drying rates per volume. Droplet falling speed also rises tremendously with diameter. A ten-fold increase for instance, in droplet diameter would lead to a 1000-fold increase in its initial velocity and approximately a ten-fold increase in its terminal velocity (neglecting diameter reductions due to drying). Hence, for the same feed and process/equipment design conditions, a higher inlet air temperature is required to bring larger-sized droplets to desired outlet particle moisture contents. This leads to over-drying of smaller droplets; lower powder production rates and hence profit levels as the plant operates well-below the maximum permissible product moisture content;

and higher energy consumption. Moreover, there is a drop in overall product quality due to increased heat load on the smaller droplets and increased production of fines, with its attendant fire and explosion risks. Consequently, monodisperse droplet generation is critical to energy-efficient spray drying operations for high-quality products.

Monodisperse droplet generation for spray drying using piezoelectric-actuated atomizers is a relatively new technology, with previous research efforts focusing mainly on proof-of-concept and experimental studies e.g. on drying kinetics of a variety of products [4, 5, 6]. The potential for energy-efficient spray drying has been recognised [7] but not explored either theoretically or experimentally for better understanding on what improvements are possible. Kosmodemyanskii et al. [8] has shown theoretically that drying kinetics can be enhanced by monodispersity, without investigating energy savings potentials. The purpose of the current work is to explore the possibilities of energy consumption reduction using modelling and simulation. Mass and energy balances as well as droplet travel dynamic equations are developed for travelling droplets. Drying kinetics are simulated with models for skimmed milk [9], but at different critical moisture contents X_{cr} (related to crust formation) to simulate different degrees of hindrance to drying (falling rate). The lower extreme $X_{cr}=0$, implies a continuously constant drying rate (as experienced by pure water). The model determines the evolution of drying gas and product state variables: temperatures T_G and T_p (°C), droplet moisture contents X and Y (kg/kg db), droplet travel speed U_p (m/s), and diameter, D_p (m). Different runs of a cylindrical dryer of given length L (m) and diameter D_D (m) are simulated to determine the drying gas inlet temperature T_{Gin} for which the same moisture outputs are realised for a monodisperse and polydisperse system. Based on [8], the polydisperse system is simulated as a monodisperse system with the largest droplet diameter in its size distribution. This simplification represents the best polydisperse system. Hence, any observed energy efficiency improvement represents the least improvement possible for the stated conditions and scale of operation.

2. Mathematical model

2.1. Heat balances

Gas and product average temperature T_G and T_p vary with droplet travel distance z by

$$\frac{dT_G}{dz}=\frac{f_p}{GC_{pG}}\left[M_{pd}\frac{dX}{dz}\left(h_{fg}+C_{pv}\left(T_G-T_p\right)\right)-\frac{1}{U_p}\pi hD_p{}^2\left(T_G-T_p\right)\right] -\frac{1}{C_{pG}}\left(h_{fg}+C_{pv}T_G\right)\frac{dY_G}{dz}-\frac{1}{GC_{pG}}\left(\pi D_D U_{loss}\left(T_G-T_{amb}\right)\right) \tag{1}$$

$$\frac{dT_p}{dz}=\frac{\pi hD_p{}^2\left(T_G-T_p\right)+M_{pd}U_p\left(h_{fg}+C_{pv}T_G-C_{pw}T_p\right)\frac{dX}{dz}}{M_{pd}U_p\left(C_{pd}+XC_{pw}\right)} \tag{2}$$

2.2. Mass balances

The average product moisture content and gas humidity are respectively given by

$$\frac{dX}{dz}=-\left(\left(\left(X\le X_{cr}\right)\left(\frac{X-X_{EQ}}{X_{cr}-X_{EQ}}\right)\right)+\left(X>X_{cr}\right)\right)\frac{h\pi D_d{}^2\left(T_G-T_p\right)}{h_{fg}M_{pd}U_p} \tag{3}$$

$$\frac{dY_G}{dz}=-\frac{f_p}{G}M_{pd}\frac{dX}{dz} \tag{4}$$

where, the first term in 3 (in the overall brackets) is the relative drying rate, based on the characteristic curve drying model for skimmed milk [9]The second term represents the drying rate during the constant-rate period. The heat transfer coefficient h is determined from the Ranz-Marshall Correlation, while the equilibrium moisture content X_{EQ} is based on the GAB sorption isotherm model.

The droplet shrinkage rate is proportional to the drying rate until X_{cr} [10].

$$\frac{dD_p}{dz} = \frac{2M_{pd}}{\pi\rho_w {D_p}^2}\frac{dX}{dz}\left(X > X_{cr}\right) \tag{5}$$

2.3. Droplet travel dynamics

From Newton's laws, the droplet/particle velocity evolution with travel distance z is

$$\frac{dU_p}{dz} = \frac{1}{U_p}\left[\left(1-\frac{\rho_G}{\rho_p}\right)g - \frac{3}{4}\frac{\rho_G C_D\left(U_p - U_G\right)^2}{\rho_p D_p}\right] \tag{6}$$

where ρ_G and ρ_p (both in kg/m^3) are densities of gas and droplet material, g=9.81m/s^2 the acceleration due to gravity, and C_D the drag force coefficient given in terms of Reynolds' number by the Schiller-Naumann correlation [11].

2.4. Initialisation and input specifications

The initial (or inlet) conditions for each of the state variables (1) – (6) are determined as follows: T_{Gin} and T_{pin} are set in actual processes by the gas and feed heater while X_{in} and Y_{Gin} depend on the product and gas feed conditions. D_{pin} and U_{pin} are determined from mass balances on a piezoelectric atomizer of orifice diameter D_{or} as

$$D_{pin} = \sqrt[3]{6q_p/\pi f_p} \tag{7}$$

$$U_{pin} = (2/3) f_p \, {D_{pin}}^3 / {D_{or}}^2 \tag{8}$$

where q_p is the volumetric flowrate (m^3/s) of the feed through the atomizer orifice. The gas mass flowrate, as set by a flow controller determines the air velocity U_G as it flows through the drying chamber, and is given as

$$G = \frac{1}{4}\rho_G U_G \pi {D_d}^2 \tag{9}$$

The system of differential equations so derived are solved in MATLAB using the explicit Runge-Kutta method [12]. Some input and parameter values used in the calculations are as given in Table 1.

Table 1. Inputs and parameters used in the simulations.

C_{pG} (kJ/kg K)	C_{pv} (kJ/kg K)	C_{pw} (kJ/kg K)	D_D (m)	h_{fg} (kJ/kg)	L (m)	q_p (m^3/s)
1	1.86	4.2	0.08	2500	6	4.17E-8
ρ_{pd} (kg/m3)	ρ_G (kg/m3)	ρ_w (kg/m3)	T_{amb} (°C)	U_G (m/s)	U_{loss} (kW/m2k)	X_{in} (kg/kg)
1500	1.2	1000	30	1	5.00E-04	4

2.5. Energy consumption analysis

The thermal energy consumption Q_{in} of a dryer per second, is the heat used in heating the drying gas from ambient T_{amb} to the required inlet temperature T_{Gin}, given by

$$Q_{Gin} = GC_{pG}\left(T_{Gin} - T_{amb}\right) \tag{10}$$

The droplet diameter is varied by setting generation frequency f_p to different values, while maintaining the feed volumetric flowrate at the same value (see equation (7)). Values of f_p = 0.5, 1, 5, 10, 100 and 640 kHz yield initial diameters of 541, 430, 251, 200, 92 and 50 μm respectively for the given feed flowrate. For a given drying gas mass flowrate *G* and other stated process and equipment conditions, the system is simulated to calculate the value of T_{Gin} that satisfies stated constraints (5±0.5%) on the product outlet moisture content for each of the droplet diameters. This gives a measure of the energy requirement (see equation (10)).

To quantify the energy savings due to monodispersity, the D_p = 50 μm case is taken as a reference D_{pref}, and the other higher diameters taken as larger droplet diameters in a polydisperse system. The percentage energy savings is thus derived from (10) as

$$S_{\%} = 100\ \left(T_{Gin\ D_p} - T_{Gin\ D_{pref}}\right) \Big/ \left(T_{Gin\ D_p} - T_{amb}\right) \tag{11}$$

An initial sensitivity analysis of the generated results showed a significant impact of the drying kinetics (particularly the critical moisture content) on the temperatures required for each droplet diameter. Not much is available in the literature in terms of critical moisture content correlations for the example product, skimmed milk. Hence, simulations were run for different values of X_{cr}, namely X_{cr}=4 (no constant-rate), 2 and 0.8 (partial constant-rate) and 0 (only constant-rate as obtainable in pure water).

3. Results and discussion

Fig. 1 shows the evolution of the state variables for the two extreme cases Xcr=0 (top) and Xcr=4 (bottom), and an intermediate case Xcr=0.8 (middle) in the drying of a stream of monodisperse droplets of initial diameter 251 μm. Overall mass and energy balances are shown to be satisfied in each case and the trends of the results are as obtainable in practice. In particular, the droplet temperature remains at approximately the wet bulb value throughout the drying period for Xcr=0 (due to constant-rate drying), while it eventually rises towards the gas temperature for Xcr=0.8. For Xcr=Xpin=4, there is no constant-rate period and so, no wet bulb droplet temperature behaviour is observed. The hindered drying behaviour, significantly increases the drying gas temperature requirement to about 350°C, compared to the cases of Xcr=0 and 0.8, which require 107°C and 150°C respectively. The slight nonlinearities observed in the moisture content evolution with height (for Xcr=0) is primarily due to non-uniform droplet velocity, and to a lesser extent, moisture accumulation in the drying air. In the three cases, the droplets start off with an initial velocity (dictated by pumping and atomization conditions) higher than the droplet property-dependent terminal value. Droplet diameter evolution is essentially linear for Xcr=0 (pure water behaviour), while for the others, the nonlinearities towards the end indicate the onset of crust formation and the attendant transition from constant-rate to falling-rate drying.

Fig. 2 shows the inlet gas temperatures required for satisfying the outlet product moisture content constraints for droplets at different diameters, as well as the percentage energy savings S% for each ratio of the generated higher droplet diameters to the reference case of 50μm. The results, which are plotted for different values of Xcr also show model fits determined by nonlinear least squares methods. The parameters of the fitting equations (12) and (13) are shown in Table 2, together with the R2 values.

$$T_{Gin} = \alpha \exp\left(\beta D_p / \left(D_p + \gamma\right)\right) \tag{12}$$

$$S_{\%} = \frac{\lambda}{1 + \phi \exp\left(-\omega D_p / D_{pref}\right)} \tag{13}$$

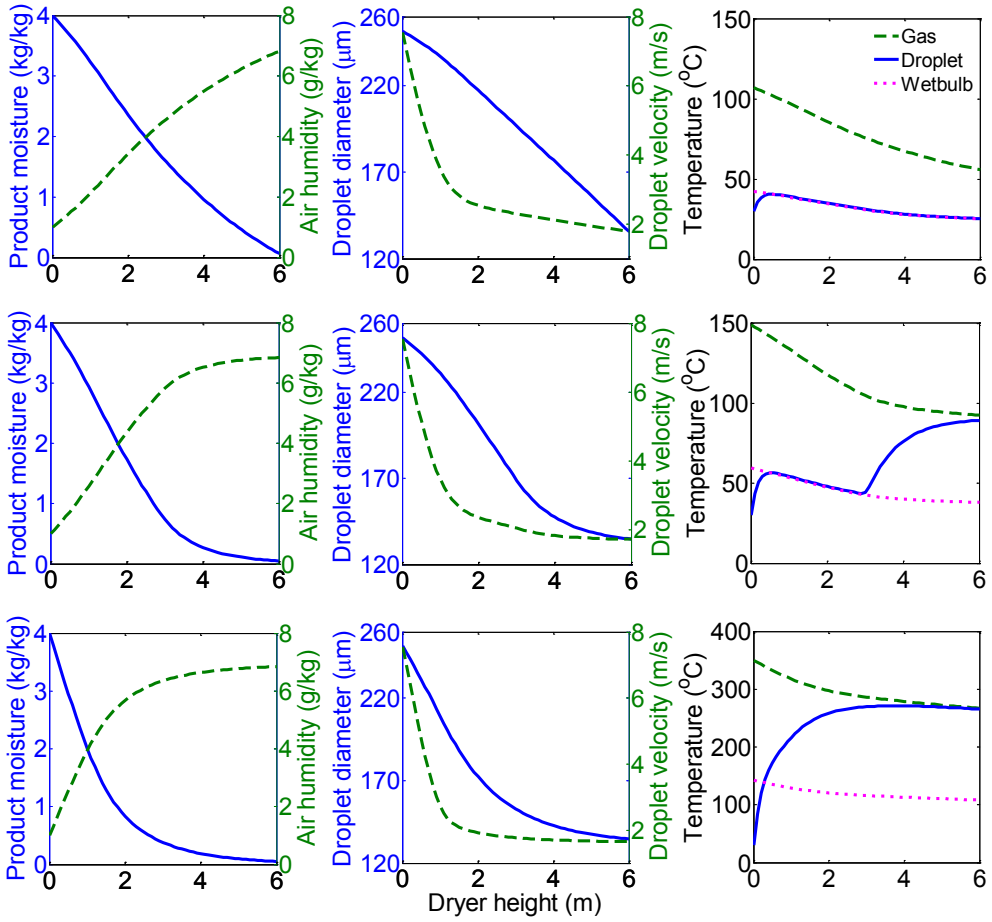

Fig. 1. Drying process behaviour for X_{cr}=0 (top), X_{cr}=0.8 (middle) and X_{cr}=4 (bottom)

Table 2. Parameter values for fitting equations (12) and (13).

X_{cr}	α	B	γ	R^2	λ	Φ	Ω	R^2
0	34.78	12.27	2.12E+03	0.9972	91.29	44.64	1.05	0.9938
0.8	41.41	10.47	1.75E+03	0.9973	89.63	59.02	1.09	0.9927
2	38.43	6.58	738.1676	0.999	92.46	12.36	0.87	0.9972
4	28.04	5.36	281.6548	0.9998	94.86	5.72	0.88	0.9982

The results of Fig. 2(a) show that as droplet diameter increases, the required inlet gas temperature also increases significantly, in an exponential fashion. This implies higher energy requirements. Hence, the percentage energy savings related to operating at the reference diameter Dpref=50μm as against higher diameters, increases with increasing droplet diameter, approaching as high as 95% as seen in Fig. 2 (b). This implies that a monodisperse system with an average droplet initial diameter of 50μm saves over 90% of the energy that would have been consumed in a polydisperse system with a desired droplet size of 50μm but which also has larger droplets, the largest

of which is 10 times as large (500μm). When the reference droplet diameter value is set higher than 50μm (not shown), this trend is maintained. The results also reveal that more hindered drying kinetics (one with higher value of Xcr) results in a higher inlet temperature requirement, for all the droplet diameters. The increased strain on the system due to the predominance of falling drying rates is felt more by the larger droplets than the smaller ones. This explains the increase in energy savings with the level of hindrance to drying (increasing values of Xcr) as shown in Fig. 2(b).

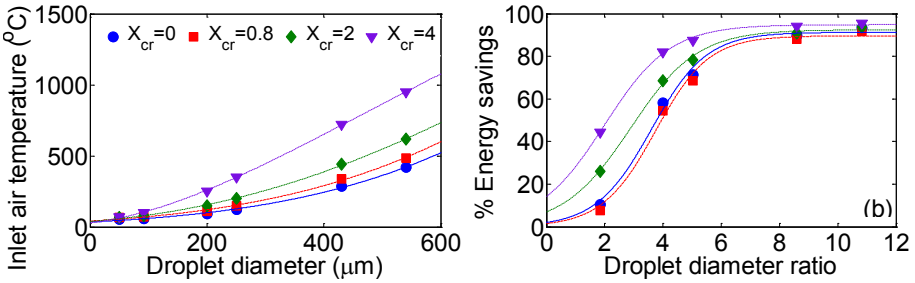

Fig. 2. (a) Required inlet gas (air) temperatures at different droplet diameters for X_{cr}=0, 0.8. 2 and 4 and (b) corresponding percentage energy savings at different ratios of maximum to reference droplet diameters. Raw results in markers are fitted to empirical models (lines)

4. Further discussion and future perspectives

A monodisperse single stream droplet drying system (Fig 3a) has been constructed at the Department of Chemical Engineering, Loughborough University. It consists of a piezoelectric-actuated inkjet print-head atomizer (a) mounted atop a glass cylindrical drying column (b) of height 6m and internal diameter 0.08m. The atomizer is driven by a signal generator and the feed pumped by a syringe pump through a heater (c) on to the print head. The drying air is supplied through a flow-straightening distributor plate, housed in (d). Droplet sizing is achieved using an adjustable camera (e) and strobe light (f) system with image analysis by the Dynamic Studio® software (Dantec Dynamics). (g) and (h) are the air heater and inlet pipe respectively. The system produces monodisperse droplets (coefficient of variation 3E-4 at release, see Fig. 3b) of required diameters using feed flowrates and droplet generation frequencies as specified in this work. Diameter measurements, up until observed droplet collisions are consistent with our simulations. Experiments are underway to validate the developed model, with refinements where necessary.

Droplet collisions and the effects of scale-up are expected to limit the energy savings practically achievable by monodisperse droplet generation to values lower than as demonstrated in the current study. However, as pointed out by [8], a polydisperse system shows a lower drying rate than a monodisperse system whose droplet diameter is equal to the maximum diameter of the polydisperse system. This is due to the faster drying kinetics of smaller droplets which creates quicker moisture accumulation in the drying air with the attendant reduction in the driving force for drying. It will therefore be interesting to understand how the interplay of these factors pan out in the overall energy behaviour of practical drying systems.

5. Conclusion

Mechanistic models of single stream monodisperse droplet dryers based on mass/heat balances and droplet travel dynamics, combined with empirical drying kinetic models have been used to quantify the energy savings opportunities associated with monodisperse droplet generation in spray drying systems. Energy savings as much as 90% are possible using a monodisperse system, compared to one that produces droplet sizes up to 10 times the desired size. Practical system limitations like droplet collision, leading to loss of monodispersity and effects of scale-up could limit the energy savings possible. However, the performance of polydisperse systems has also been somewhat overestimated in this work. Hence, it is interesting to explore how the interplay of these forces affect the practically-achievable energy savings. This would require experimental validation at lab, pilot and industrial scales.

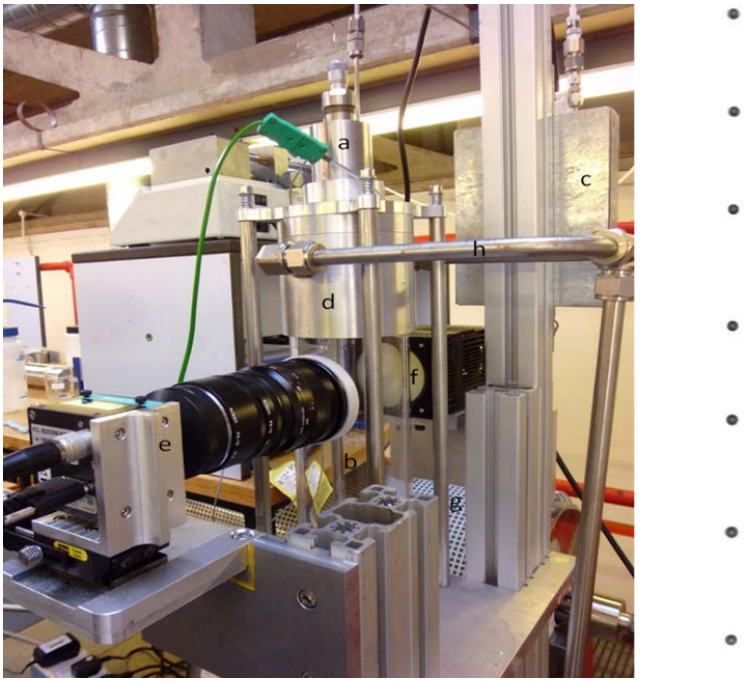

(a) (b)

Fig. 3(a). Top section of experimental single-stream monodisperse droplet dryer, labelled as follows: a: piezo-electrically-actuated atomiser housing b: glass drying column c: feed heat exchanger d: air flow straightener housing e: imaging camera f: strobe light g: air heater h: air inlet pipe. Fig. 3(b). Image of single-stream monodisperse droplets produced by atomiser.

Acknowledgements

The research leading to this paper has received funding from the European Union's FP7 programme, grant agreement no. 613732 – ENTHALPY – www.enthalpy-fp7.eu. Special thanks to Mr Anthony Eyre of the Department of Chemical Engineering, Loughborough University, who helped with the construction of the experimental monodisperse droplet single-stream drying system and TNO Netherlands for designing the piezoelectric atomiser.

References

[1] Mujumdar AS. Guide to industrial drying principles, equipment and new developments. The International Workshop and Symposium on Industrial Drying, Mumbai, India; 2004.
[2] Ramirez CA, Patel M, Blok K. From fluid milk to milk powder: Energy use and energy efficiency in the European dairy industry. Energy 2006;31;12;1984-2004.
[3] Anandharamakrishnan C, Ishwarya, PS. Spray drying techniques for food ingredient encapsulation. Oxford: Wiley Blackwell; 2015.
[4] Sadek C, Huashan L, Schuck P, Fallourd Y, Pradeau N, Le Floch-Fouere C, Jeantet R. To what extent do whey and casein micelle proteins influence the morphology and properties of the resulting powder? Dry Tech. 2014;32;13;1540–51.
[5] Rogers S, Wu WD, Lin SXQ, Chen XD. Particle shrinkage and morphology of milk powder made with a monodisperse spray dryer. Biochem Eng J 2012;62;92–100.
[6] Patel KC, Chen XD. Drying of aqueous lactose solution in a single stream dryer. Food & Bioprod Proc 2008;86;3;185–97.
[7] Van Deventer HC, Houben R, Koldeweij R. New atomization nozzle for spray drying. Dry Tech 2013;31;8;891–97.
[8] Kosmodemyanskii YV, Fokin AP, Planovskii AN. Effect of droplet size distribution on spray drying kinetics. J Eng Phys 1968;14;1;19–22.
[9] Langrish TAG, Kockel TK. The assessment of a characteristic drying curve for milk powder for use in computational fluid dynamics modelling. Chem Eng J 2001;84;1;69–74.
[10] Tsotsas E. Multiscale approaches to processes that combine drying with particle formation. Dry Tech 2015;33(15-16);1859–871.
[11] Schiller L, Naumann Z. A drag coefficient correlation. Zeitschrift des Vereins Deutscher Ing 1935;77;318–320.
[12] Shampine LF, Reichelt MW. The MATLAB ODE Suite. SIAM J Sci Comp 1997;18;1–22.